Diffusion-controlled metabolism for long-term survival of single isolated microorganisms trapped within ice crystals

Robert A. Rohde and P. Buford Price*

Department of Physics, University of California, Berkeley, CA 94720

Contributed by P. Buford Price, August 29, 2007 (sent for review July 23, 2007)

Two known habitats for microbial metabolism in ice are surfaces of mineral grains and liquid veins along three-grain boundaries. We propose a third, more general, habitat in which a microbe frozen in ice can metabolize by redox reactions with dissolved small molecules such as CO_2, O_2, N_2, CO, and CH_4 diffusing through the ice lattice. We show that there is an adequate supply of diffusing molecules throughout deep glacial ice to sustain metabolism for $>10^5$ yr. Using scanning fluorimetry to map proteins (a proxy for cells) and F420 (a proxy for methanogens) in ice cores, we find isolated spikes of fluorescence with intensity consistent with as few as one microbial cell in a volume of 0.16 μl with the protein mapper and in 1.9 μl with the methanogen mapper. With such precise localization, it should be possible to extract single cells for molecular identification.

F420 fluorescence | fluorimetry | ice cores | dissolved molecules | single cells

Until recently it was not understood how microorganisms trapped in ice obtain the water, energy via redox reactions, and bioelements such as carbon required for life. Price (1) provided part of the answer. He developed a quantitative picture of how micrometer-sized bacteria and archaea could be swept into veins in a growing ice cap, along with chemical impurities of aeolian origin that are insoluble in the ice. In equilibrium the freezing point of an aqueous solution is lower than that of pure water. In polycrystalline ice the solute ions concentrate at the triple junctions of grains, leading to a vein structure. Price calculated the molarity and the vein diameter as a function of freezing point depression for the concentration of the major solute ions in ice. Vein diameters range from $\approx$1 μm at -50°C to $\approx$10 μm at -4°C in glacial ice. Two disadvantages of this habitat are that large microbes do not fit into veins, and those small enough to fit must adapt to a harsh chemical environment such as sulfuric acid. Nevertheless, for those adapted to such an environment, redox reactions of impurities in the veins yield enough energy to sustain a substantial microbial population.

Junge *et al.* showed that many microorganisms in sea ice occupy brine channels (2) and that many in lake ice occupy veins (3). Mader *et al.* (4) showed that both bacteria and fluorescent beads added to water used to make ice are rejected from the solid phase and incorporated into liquid veins, provided that they are small enough to fit, whereas beads larger than the vein diameter are frozen into solid ice.

Tung *et al.* (5) proposed a second icy habitat, which is afforded by surfaces of mineral grains around which the freezing point of the aqueous solution is depressed within the "hydration distance." Microbes attached to minerals extract energy in redox reactions with ions in the mineral grain. Wettlaufer (6) accounted for equilibrium undercooling, $T_m - T$, as a function of thickness of the "unfrozen" water as the sum of four terms: depression of the freezing point of an ionic solution, an attractive van der Waals contribution, a Debye–Hückel contribution due to charges on the mineral surface, and a Gibbs–Thomson contribution, which is a function of curvature of the walls of any pores present. In the case of clay grains, the thickness of the unfrozen layer decreases from tens of nanometers at temperatures near 0°C to $\approx$0.3 nm at -80°C (7). Experiments (8, 9) have shown that the unfrozen water still has considerable mobility at these low temperatures. Price and Sowers (10) have presented evidence for microbial metabolism at temperatures as low as -40°C (water activity $a_w = 0.72$).

Up to 95% of the 10^8 to 10^{10} cells per cm^3 in the basal ice cored from a depth of 3,041–3,054 m in the Greenland Ice Sheet Project 2 (GISP2) are attached to clay grains (5). At four depths, Miteva *et al.*[†] found that up to $\approx$85% were alive. Reasoning from their observed linear correlation of the number of cells per grain with grain circumference and from the factor of $\approx 10^4$ higher electronic conductivity parallel to the basal plane than perpendicular to it in Fe-rich clays (11), Tung *et al.* (5) inferred that the majority of the attached cells were Fe reducers metabolizing by electron shuttling. With this mechanism, they were able to explain how Fe reducers could reduce nearly 100% of all Fe^{3+} in clay grains. With epifluorescence microscopy of F420 [an autofluorescing coenzyme that is accepted as a unique signature of methanogens (12)], they determined that $\approx$2.4% of the cells in the basal ice were methanogens.

Need for a Third Microbial Habitat in Ice

Although the veins and mineral surfaces provide habitats for many microbes, observations suggest that these are unlikely to be the only locations where life endures in glacial ice. Numerous papers report the identification of microbes of diverse taxa, including nonextremophiles in ice (13–22). Eukarya up to $\approx 10^2$ μm in size, some of which are viable, have been found in glacial ice (23–27). Because glacial ice is coldest at or near the top, the veins formed during grain growth and recrystallization will be the smallest in diameter and have the highest ionic concentration there. One might expect then that only extremophiles and the smallest microbes would be able to survive this harsh environment.

Baker *et al.* (28) and Barnes and Wolff (29) used scanning electron microscopy with energy-dispersive x-ray spectroscopy to map the location and composition of soluble impurities in glacial ice. Barnes and Wolff detected veins only at depths where the bulk concentration of ions (mainly sulfate) was greater than $\approx$1.6 μM and where the bulk ice was acidic. They suggested that vein networks do not form unless the acidic impurities are

Author contributions: P.B.P. designed research; R.A.R. and P.B.P. performed research; R.A.R. and P.B.P. analyzed data; and R.A.R. and P.B.P. wrote the paper.

The authors declare no conflict of interest.

Abbreviations: GISP2, Greenland Ice Sheet Project 2; WAIS, West Antarctic Ice Sheet.

*To whom correspondence should be addressed. E-mail: bprice@berkeley.edu.

[†]Miteva, V., Sowers, T., Brenchley, J. E. (2005) 11th International Symposium on Microbial Ecology (ISME-11), Vienna, Austria, August 20–25, 2006.

This article contains supporting information online at www.pnas.org/cgi/content/full/0708183104/DC1.

sufficient to coat all grain boundaries with at least a monolayer. Baker *et al.* (28) found that veins are present only in interglacial-stage ice, where the bulk pH is acidic. Thus, veins as a microbial habitat may be absent in ice with low acidity or large grain size.

Experimental evidence for the presence of both aerobes and anaerobes at the same depth in glacial ice provides a further constraint on habitat. Sheridan *et al.* (13) and Miteva *et al.* (14) identified a rich variety of both aerobes and anaerobes at the same depth, 3,043 m, in a sample of GISP2 ice. Using scanning fluorimetry to scan GISP2 ice cores at the National Ice Core Laboratory (NICL), we recently found that anomalously high levels of both $\delta^{18}O_{air}$ (30) and CH_4 (31) at the same depth, 2,672 m, corresponded to excess microbial concentrations localized within a 1-cm^3 ice volume.[‡] We concluded that these gas anomalies are the waste products of both aerobic respiration and methanogenic metabolism within the same community. Because methanogens are among the most strictly anaerobic microorganisms and will not grow or make CH_4 in the presence of oxygen (32), this suggests that obligate aerobes and methanogens must have access to separate, isolated microenvironments within the same ice, rather than coexist in veins.

In view of all these limitations, we propose a third icy habitat that can accommodate microbial members of all three domains, of any size, at all depths, independent of oxygen content in the ice. In the next section, it will become clear that the habitat is so confining that it cannot permit movement or growth, but only survival.

Habitat 3: Interior of an Ice Crystal Far from Veins and Grain Boundaries

It is not obvious that a habitat in solid ice would permit survival, to say nothing of movement or growth. To set the stage, we model the behavior of a single methanogen frozen into the interior of an ice crystal at a temperature −10°C. For GISP2 ice, this corresponds to a depth ≈3,000 m and pressure of ≈30 MPa. In equilibrium at −10°C, an isolated cell will be coated with ≈1 nm of unfrozen water (33), which provides easy access of nutrient molecules to the cell membrane. We take the mass per cell to be 38 fg for cells of the average size measured by examining SEM micrographs of cells from the deep GISP2 ice core (5). That mass corresponds to ≈10^9 carbon atoms and a radius of ≈0.21 μm for a cell of spherical shape. Price and Sowers (10) found that the typical rate of carbon turnover for survival metabolism in a microbial community at −10°C is 2×10^{-6} g C·(g C)$^{-1}$·yr^{-1} (in which g C is grams of carbon), which would require only ≈1,900 carbon atoms to be converted from CO_2 to CH_4 per cell per year to repair molecular degeneration, assuming the reaction

$$4H_2 + CO_2 \rightarrow CH_4 + 2H_2O. \quad [1]$$

A methanogen in ice could thus be a sink for dissolved H_2 and CO_2 molecules and a source of CH_4 and H_2O molecules. The CH_4 would be trapped in the ice but could diffuse short distances.

To determine whether the reaction in **1** can be sustained in ice at the rate of 1,900 molecules per year per cell, we need to know the equilibrium concentrations of CO_2 and H_2 dissolved in ice and the diffusion coefficients of CO_2, H_2, CH_4, and H_2O in ice at −10°C. Later we will generalize the discussion to metabolism of cells of larger size, at other temperatures, for other redox reactions, including aerobes and anaerobes. Supporting information (SI) Table 1 gives the measured or estimated diffusion coefficient, D, within an ice crystal lattice (as distinct from diffusion along veins and grain boundaries, which is much faster) for a number of atoms and molecules. All of the gas molecules relevant to climate studies have values of $D \leq 10^{-14}$ m^2·s^{-1}, consistent with survival of observed sharp changes of concentration on timescales >10^5 yr. SI Table 2 gives equilibrium concentrations of dissolved molecules in the ice lattice, under the assumption that the gases in the ice are in equilibrium with air bubbles in the ice.

As a result of snow densification and pore closures in glacial ice, ≈10% of the firn volume becomes trapped in ice as air bubbles. At sufficiently high pressures, the bubbles become unstable against transformation into the air-hydrate clathrate phase (34). Lipenkov (35) reviewed the measurements of sizes and concentrations of air bubbles and of air-hydrate crystals as a function of depth in the Vostok ice core, and Pauer *et al.* (36) did the same for air in the Greenland Ice Core Project (GRIP) core. Due to the long duration for nucleation and growth of an air-hydrate crystal at a bubble, air-hydrate crystals and bubbles coexist at depths ≈500 to ≈1,250 m in Vostok ice and at ≈650 to 1,300 m in GRIP ice. Lipenkov (35) concluded that the conversion efficiency is one air-hydrate crystal per air bubble. For depths shallower than the air-hydrate phase boundary, the equilibrium molar fraction, C_e, of gas in the ice lattice is proportional to pressure, as given in SI Table 2. For greater depths, C_e is approximately constant and equal to the concentration at nucleation (37).

Diffusion of gases dissolved in the ice lattice has been experimentally observed in a number of situations, including: diffusion of gas from small bubbles to larger bubbles, diffusion from bubbles to air-hydrate crystals, and diffusion from small hydrate crystals to large ones (37). Further, each of these observed processes can be understood as the result of a slowly diffusing gas seeking the state of lowest free energy. From measurements of relative sizes of air-hydrate crystals at typical separations of ≈1 mm and at depths 1,350 to 2,040 m, Uchida *et al.* (37) obtained an average value of the product of the diffusion rate, D, and the equilibrium molar fraction, C_e, as $DC_e \approx 10^{-19}$ m^2·s^{-1} at a temperature of −40°C. This is consistent with the values from SI Tables 1 and 2 for oxygen and nitrogen and implies a gas mobility of several tens of centimeters per 10^5 yr.

Time for Replenishment of Molecules Reacted During Metabolism of an Isolated Cell

We now show that an isolated microbial cell of volume V_{cell} in an ice lattice can metabolize at the rate $\mu(T)$ [in g C·(g C)$^{-1}$·yr^{-1}] necessary for survival (10) by using suitable impurities that are present in equilibrium concentration C_e (in mole fraction) and that diffuse through the ice with diffusion coefficient $D(T)$. Diffusion is governed by the equation

$$\frac{\partial C(\vec{x}, t)}{\partial t} = D(T)\nabla^2 C(\vec{x}, t). \quad [2]$$

By enforcing spherical symmetry and matching boundary conditions, an exact steady state solution to this can be found as

$$C(r) = C_e\left(1 - \frac{r_{cell}}{r}\right), \quad [3]$$

with r_{cell} denoting the radius of the cell. It follows that the number of molecules entering a spherical cell per unit time is $4\pi D(T)C_e r_{cell}\rho_{ice}/MW_{ice}$, where ρ_{ice} and MW_{ice} are the density and molecular weight of ice. Equating this to the metabolic requirements of the cell, we find that for a given metabolic rate, diffusion rate, and equilibrium concentration, the largest sustainable cell is given by

$$r_{cell} = \sqrt{\frac{3D(T)C_e}{\mu(T)}\frac{MW_{carbon}}{MW_{ice}}\frac{\rho_{ice}}{\rho_{cell}}} \approx 1.35\sqrt{\frac{D(T)C_e}{\mu(T)}}. \quad [4]$$

[‡]Price, P. B., Rohde, R., Bramall, N., Bay, R. (2006) *Eos Trans Am Geophys Union Fall Meeting Suppl* 87:U43B-0868.

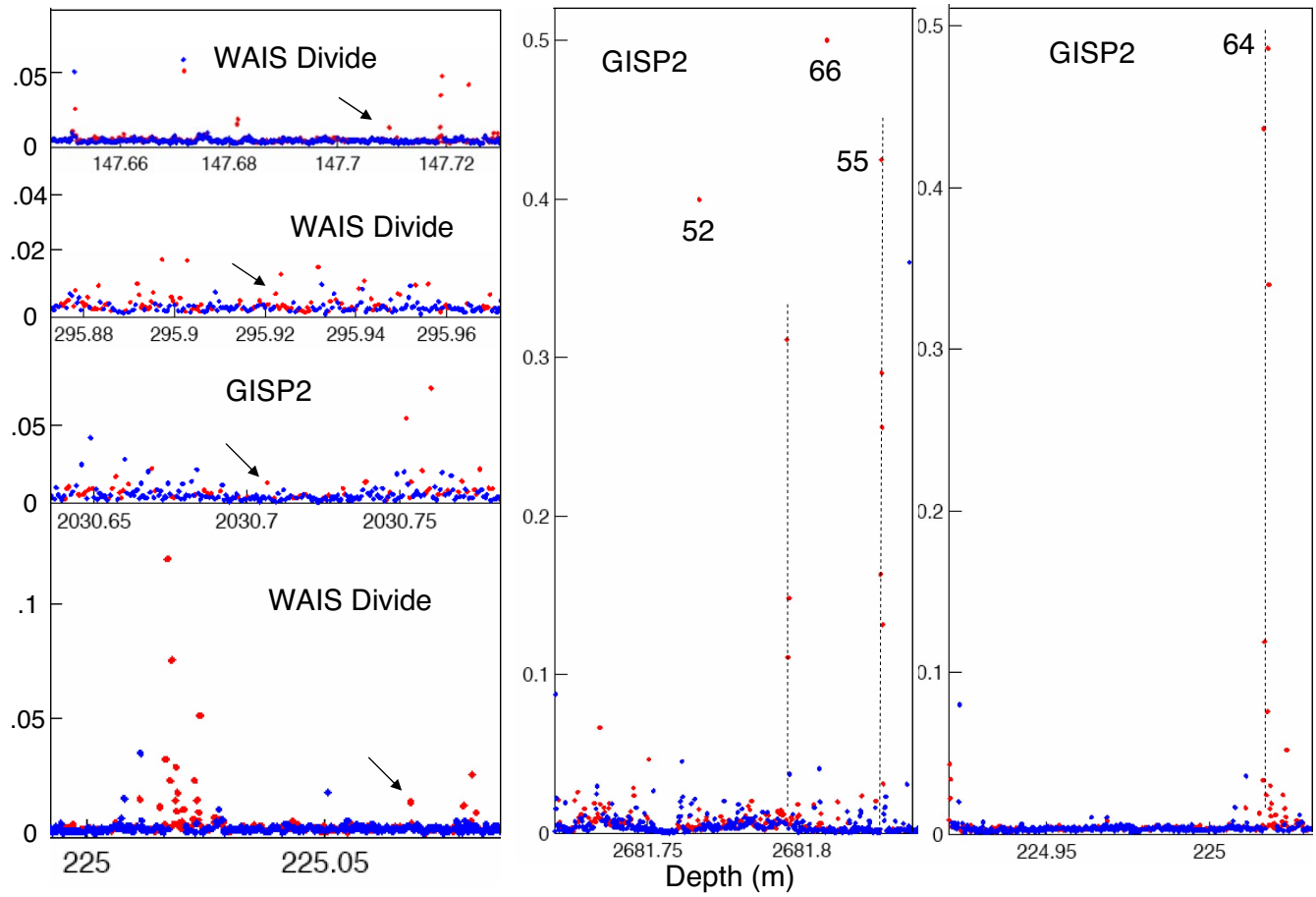

Fig. 1. Examples of protein fluorescence intensity vs. depth obtained with the TUCS in scans of ice cores from WAIS Divide (Antarctica) and GISP2 (Greenland). Red points have spectra consistent with protein fluorescence.

Consider metabolism (**1**) at −10°C by methanogens at a rate $\mu(-10°) = 2 \times 10^{-6}$ g C·(g C)$^{-1}$·yr^{-1} (10) at a 3,000-m depth in GISP2 ice. For a typical 38-fg cell (5), this corresponds to a consumption of only 1,900 C atoms per year. As 3,000 m is far below the clathrate transition zone, the equilibrium concentration is determined by the clathrate dissociation pressure (6.2 MPa at −31°C). From SI Table 1, $D(CO_2) = 10^{-14}$ m^2·s^{-1}, $C_e(CO_2) = 8 \times 10^{-10}$ moles·mole$_{ice}^{-1}$·MPa^{-1} $= 5 \times 10^{-9}$ moles·mole$_{ice}^{-1}$, and $D(H_2) = 1 \times 10^{-8}$ m^2·s^{-1}. For hydrogen, we note that air containing ≈550 ppb of H_2 has too low a concentration to reach the equilibrium with bubbles described in SI Table 2, meaning that essentially all of the H_2 available in air becomes dissolved in the ice. Given that glacial ice at the elevation of GISP2 forms with ≈9% air by volume (38), this gives $C(H_2) = 4 \times 10^{-11}$. From SI Table 1 we see that the products H_2O and CH_4 will diffuse out of the shell at rates comparable to that of CO_2, so that the waste products do not build up around the cell. From these values we see that methane production is limited by the abundance of CO_2 and from Eq. **4** that cells with a diameter as large as 76 μm will receive sufficient CO_2 to sustain survival metabolism. Hence, this accommodates archaea, bacteria, and even quite large eukaryotes.

At a depth of 100 m (1 MPa) where the temperature is much lower (−32°C), the metabolic rate is $\mu(-32°) = 5 \times 10^{-8}$ g C·(g C)$^{-1}$·yr^{-1} (10) or a turnover rate of only 48 carbon atoms per year for the typical cell. We get from SI Tables 1 and 2 that $D(CO_2) = 10^{-15}$ m^2·s^{-1} and $C_e(CO_2) = 8 \times 10^{-10}$ moles·mole$_{ice}^{-1}$, which accommodates cells up to 60 μm in diameter. In this example, the lower diffusion rate at −32° is largely compensated for by the lower metabolic requirements.

For other taxa, metabolism can proceed at the rate given by Price and Sowers (10), provided diffusion is rapid enough to maintain the supply of reactants. Examples include aerobic respiration (e.g., $CH_4 + 2O_2 \rightarrow 2CO_2 + 2H_2O$), nitrogen fixation ($N_2 + 6H^+ + 6e^- \rightarrow 2NH_3$), and carbon monoxide oxidation (e.g., $O_2 + CO \rightarrow CO_2$), all of which involve small molecules with values of D not smaller than $D(CO_2)$ (SI Table 1). N_2, O_2, CH_4, and CO are relatively abundant in the atmosphere: 565 ± 200 ppbV for CH_4 (39) and 100 ± 50 ppbV for CO (40). All of them form clathrate hydrates with known phase diagrams, and their solubilities in ice as a function of temperature can be estimated from their dissociation pressures (41–43). We conclude that the above metabolic processes should not be restricted by the values of D or C_e.

As a final example, we consider aerobic consumption of CH_4 at 3,000-m depth and −10°C. The maximum size cell that can respire aerobically at 2×10^{-6} g C·(g C)$^{-1}$·yr^{-1} via a reaction such as $CH_4 + 2O_2 \rightarrow CO_2 + 2H_2O$ can be estimated with D assumed to be 10^{-14} m^2·s^{-1} and C_e for methane assumed to be 4×10^{-11} moles·mole$_{ice}^{-1}$ (limited by atmospheric abundance). This allows a spherical cell with diameter as large as 5 μm to metabolize at a survival rate at −10°C. Even if D were as low as 10^{-15} m^2·s^{-1}, a concentration of methane near a cell 1.6 μm in size could sustain survival metabolism.

Sustainability of Intraglacial Metabolism

The last factor to consider is whether metabolism by diffusion through glacial ice can be sustained for the entire age of the ice.

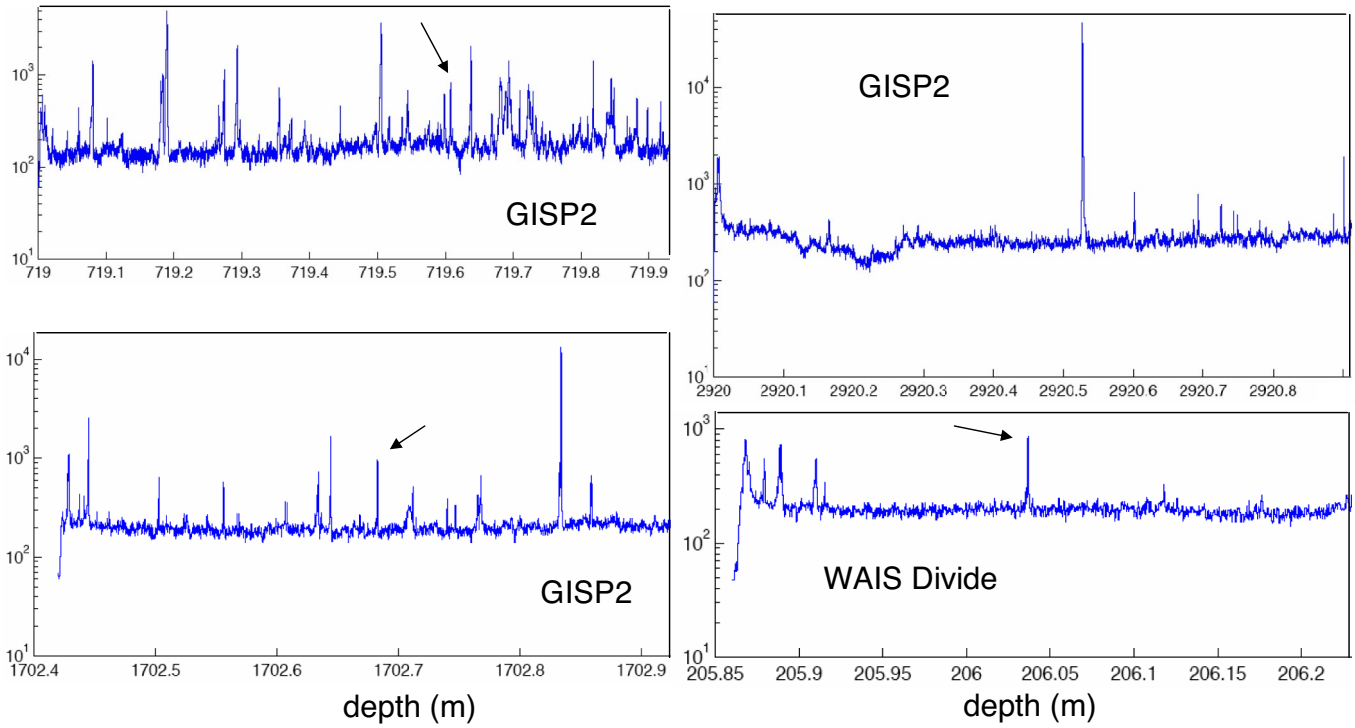

Fig. 2. Examples of F420 fluorescence intensity vs. depth obtained with the F420-fluorimeter.

For a given metabolic rate and concentration of microbes, we can approximate the time required to deplete the reactants as $2C_e\rho_{ice}MW_{carbon}\,[n_{cell}\,m_{cell}\,\mu(T)\;\;A\,MW_{ice}]^{-1}$, where n_{cell} is the number density of cells, m_{cell} is the mean mass per cell, and A is the number of moles of reactant per mole of carbon metabolized. For a lifetime τ, this can be recast to note that the sustainable concentration of cells is approximately

$$n_{cell} \approx \left(1.2\,\frac{g}{cm^3}\right)\frac{C_e}{A\,\mu(T)m_{cell}\tau}. \qquad [5]$$

For $\tau \approx 100$ kyr, cells of mass 38 fg, a metabolic rate of 10^{-6} g C·(g C)$^{-1}$·yr^{-1} at −10°C (10), a concentration of $\approx 4 \times 10^{-11}$ moles·mole$_{ice}^{-1}$ (the case for hydrogen and methane), and $A = 4$ from reaction **1**, we find that the supportable population of methanogenic archaea by diffusion to isolated cells is ≈2,000 cm^{-3}. An additional ≈8,000 small cells per cm^3 are supportable via aerobic methane consumption. These estimates are conservative in that they ignore the period spent at lower temperature, which would increase the sustainable population size, due to the lower metabolic rate.

Fluorimetric Evidence for Isolated Single Microbes

We used two new scanning fluorimeters to search for evidence for the existence of isolated microbes in ice cores stored at −36°C at NICL. To map microbial cells via their protein autofluorescence (dominated by protein-bound tryptophan), we used a Photon Systems (Covina, California) TUCS (Targeted UV Chemical Sensor) fluorimeter with a 224-nm laser source. The cylindrical volume sampled has a radius ≈100 μm and depth ≈0.5 cm governed by the laser beam diameter, depth of focus, and acceptance of the six phototubes. To map the coenzyme F420 in methanogens, we used a compact 404-nm laser fluorimeter of our own design, which samples a volume with radius ≈350 μm and depth 0.5 cm. The two instruments take readings at ≈300-μm depth intervals.

Fig. 1 shows protein fluorescence as a function of depth in several regions of West Antarctic Ice Sheet (WAIS) Divide and GISP2 ice cores. Red points have spectra consistent with protein fluorescence; blue points have a different spectral shape. Four of the high points are labeled by numbers indicating the number of cells with an average mass of 38 fg within an illuminated spot.

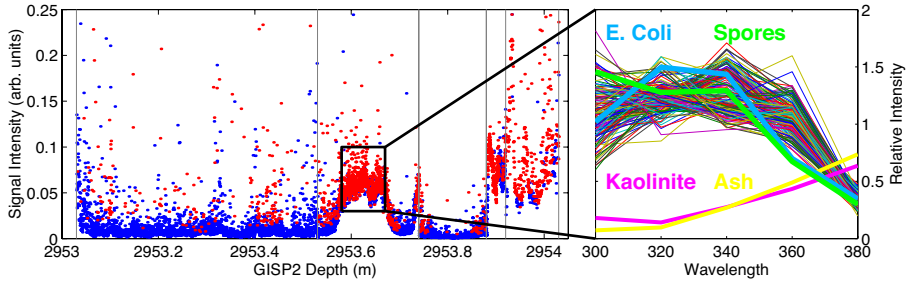

Fig. 3. Calibration of TUCS to microbes in ice. (*Left*) Intensity of fluorescence in the TUCS along a 1-m section of GISP2 ice. Points in red indicate protein fluorescence; points in blue have spectra inconsistent with proteins and are likely inorganic. (*Right*) Spectra for measurements in the boxed region compared with spectra for lab specimens for bacteria and minerals.

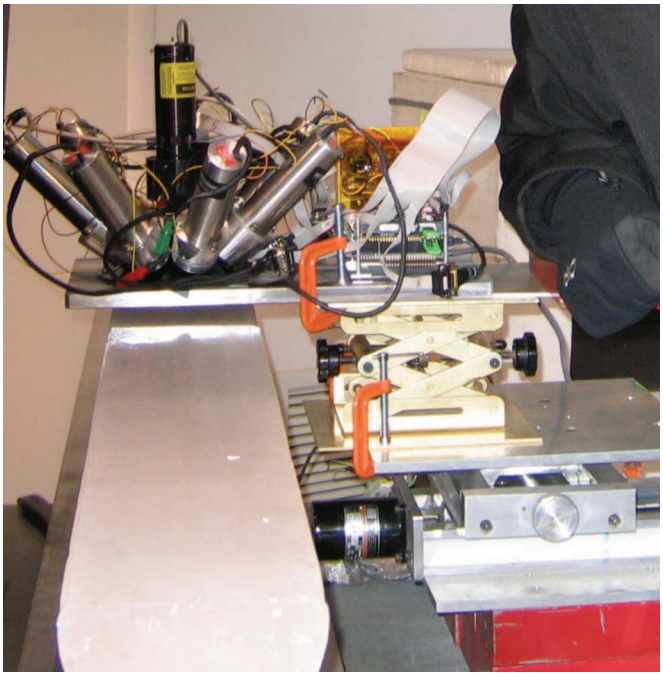

Fig. 4. F420 fluorimeter with 404-nm laser (vertical black cylinder) surrounded by seven photon counters covered by band-pass filters, fixed at an adjustable height above an ice core on a translation stage.

The high fluorescence intensity in the spot suggests that the laser beam passed through a vein containing a high concentration of microbes. At three depths where several points with high intensities fall close to a vertical dotted line, the laser beam may have traversed a vein at a small angle, resulting in excitation of protein fluorescence several times. Several points marked with an arrow indicate signals with intensity consistent with fluorescence of single microbes. Points with higher and lower intensity are likely due to microbes with higher and lower protein concentrations, surviving in the ice lattice as isolated cells. Such points provide our best evidence that isolated cells not associated with veins exist in glacial ice.

Fig. 2 shows the F420 fluorescence intensities in several regions of WAIS Divide and GISP2 ice cores. Arrows indicate several spikes with intensity corresponding to that of a single 38-fg methanogenic cell.

Discussion

We have developed a quantitative underpinning for a habitat for isolated microbes in solid ice and presented evidence, via scanning fluorimetry, that microbes occupy this habitat. We showed that at all depths there is an adequate concentration of small molecules of atmospheric origin dissolved in the ice lattice and available for metabolism by isolated microbes. At shallow depths, small air bubbles shrink by diffusion of gases from their surfaces to larger bubbles, driven by the Gibbs–Thomson effect. At depths where all air bubbles have converted to air-hydrate crystals, their rate of change of size with depth (i.e., time) provides an adequate supply of dissolved gases to meet the needs of the very slow metabolism expected of microbes frozen into the ice, even for a time $>10^5$ yr.

Using our scanning fluorimeters, we mapped microbial distributions and methanogen distributions at 300-μm depth intervals in a number of ice cores. The data suggest that microbes in both Greenland and Antarctic ice have a broad distribution of cell sizes. The results support our calculations that microbes up to at least 5 μm in diameter survive in the ice lattice, even if far from veins and mineral surfaces.

The proposed habitat avoids problems associated with the vein habitat, including the toxicity of reactants in veins, their narrow width, their lack of continuity throughout glacial ice, and the presence or absence of free oxygen in veins. With an equilibrium concentration of 2.4×10^{-7} mole fraction O_2 dissolved in the lattice, both aerobes and anaerobes should survive as isolated cells in the lattice. Because this might not be obvious, we elaborate: An isolated aerobe can respire by diffusion of O_2 and CH_4 molecules from the ice lattice to its cell membrane. Low levels of the enzymes catalase and superoxide dismutase have been detected in methanogens (44, 45), and these may serve as adequate protection against the toxic products of oxygen reduction at that low concentration of O_2.

One might ask how nonpsychrophiles can survive when incorporated into the ice lattice at an ambient temperature as low as −55°C (in East Antarctic ice) and at a hydrostatic pressure that may exceed ≈30 MPa at the bottom of a growing ice sheet. Smith *et al.* (46) showed that after 2 months of exposure in the Southern Ocean, several taxa of mesophiles including *Escherichia coli* were able to grow at −1.8°C and 34.5 ppt salinity and were no longer able to form colonies at 37°C (their previous optimal growth temperature). Sharma *et al.* (47) discovered that *E. coli* and *Shewanella oneidensis* remain viable and motile in liquid veins in ice for more than 1 month at pressures up to 1,600 MPa. These and other experiments show that nonpsychrophiles deposited onto a growing ice cap may adapt to both low temperatures and high pressures.

The requirement that the molecules have sufficiently high diffusivity and equilibrium concentration in solid ice to maintain metabolism for more than 10^5 yr rules out polyatomic molecules with more than about five atoms: Methane will work but acetate has too low a diffusivity. One might ask whether microbes that prefer large molecules for their metabolism and that grow best in the presence of catalysts can live isolated in ice with access only to small molecules. Faced with the necessity of doing without, such microbes may express genes that allow them to use an alternative source such as methane + oxygen.

We have shown that values of $D \approx 10^{-15}$ to 10^{-14} $m^2 \cdot s^{-1}$ are sufficiently high to sustain metabolism at all depths in glacial ice. Conversely, using the expression $x \approx (Dt)^{1/2}$ to estimate diffusion distance in time t, and values of D in SI Table 1, we see that initially sharp profiles in ice of gases used in studies of climate change (CO_2, CH_4, N_2O, HDO, and $H_2{}^{18}O$) will be blurred by no more than a few cm on a timescale of 10^5 yr.

It is worth reiterating that in solid ice, microbial cells survive at a metabolic rate just great enough to repair macromolecular damage, which is ≈6 orders of magnitude lower than that necessary for exponential growth and mobility (10). Thus, the problem of carving out room for cell division in the ice does not arise.

It may be possible to exploit the ability of the TUCS scanning fluorimeter to localize single cells within its active volume of 160 nl. Westphal *et al.* (48) have developed a method to extract micrometer-sized interplanetary dust grains from an aerogel target on the National Aeronautics and Space Administration Stardust mission by using a "nanomanipulator" to cut out a small portion of the aerogel containing the grain. Such a device could be used in a cold room to cut out the volume of ice associated with a given fluorimeter signal. Then, under sterile conditions, the ice could be melted, and a single-cell genetic analysis could be done (49) on one or more cells located with the fluorimeter.

Materials and Methods

We assume that intensities of protein and F420 fluorescence per cell are independent of time for living microbes in ice, on the

grounds that their survival metabolism is sufficient to repair macromolecular damage (10).

With the TUCS we did ground truth calibrations at depths 2,953.6, 2,953.95, 3,000, 3,018, and 3,035.88 m in GISP2 by comparing fluorescence intensity, I_{TUCS}, with counts of stained cells (50). We obtained the following conversion factors: Assuming an average cell mass of 38 fg (5), the background level for the TUCS fluorescence signal corresponds to $\approx$0.5 to $\approx$1.4 cell; the number of cells detected in the active cylindrical volume of depth 0.5 cm is $243 \times I_{TUCS}$; and the concentration is $C_{cells} = 1.52 \times 10^6\ cm^{-3} \times I_{TUCS}$. Fig. 3 (*Right*) shows five-channel fluorescence spectra of *E. coli* (green curve), *Bacillus* spores (blue), kaolinite grains (pink), and volcanic ash (yellow) measured with the TUCS. Protein fluorescence is characterized by having the highest intensity at 320 and 340 nm. Fluorescence of mineral grains is several orders of magnitude weaker than that of microbial cells and usually has maximum intensity at wavelengths >380 nm. The curves for kaolinite and ash are scaled up by a factor 100 for visibility. Fig. 3 (*Left*) shows TUCS intensity at 300-μm depth intervals at a depth of 2,953.9 m in a 1-m-long GISP2 ice core chosen for calibration purposes because Tung *et al.* (50) had found a huge excess of microbial cells including methanogens in a 20-ml sample from that depth. The full spectra for every point are stored on disk. The points in red are for spectra with shapes that correspond to protein fluorescence. The points in blue have different emission spectra, probably due to mineral dust grains in the ice.

Fig. 4 shows our F420 fluorimeter in position to scan an ice core. It uses a 404-nm laser to excite F420 fluorescence in a volume $1.9 \times 10^{-3}\ cm^3$. To calibrate this instrument, we did scans along the same regions of GISP2 ice cores with very high microbial concentrations where Tung *et al.* (50) counted methanogens with epifluorescence microscopy. We found that the background level corresponds to 0.15 to 0.3 methanogenic cell of mass 38 fg. The number of methanogens detected in the active volume is $1.94 \times 10^{-3} \times I_{F420}$, and the concentration is $C_{meth} = 1.02\ cm^{-3} \times I_{F420}$. We note that F420 fluoresces only if it is in an oxidized state and if its pH is greater than 6 (51). During metabolism, 80% of F420 is in the oxidized state (52). When the cell stops metabolizing, the amount of oxidized F420 decreases; thus, F420 fluorescence is an indicator of active methanogenesis. The concentration of F420 in a living methanogen depends not only on its cell mass but also to some extent on its species (53).

We thank Ryan Bay for help with electronics and Nathan Bramall for his contributions to optical design and for his measurements of fluorescence spectra of microbial taxa and mineral species. We thank Eric Wolff and Florent Dominé for helpful discussions, Boonchai Boonyaratanakornkit for preparing methanogens for us to use in calibrating the F420 fluorimeter, and Riccardo Cavicchioli and Adrian Ponce for critical reviews. This research was supported in part by National Science Foundation Grant ANT-0440609.

1. Price PB (2000) *Proc Natl Acad Sci USA* 97:1247–1251.
2. Junge K, Eicken H, Deming JW (2004) *Appl Environ Microbiol* 70:550–557.
3. Junge K, Deming JW, Eicken H (2004) in *Bioastronomy 2002: Life Among the Stars*, eds Norris RP, Stootman FH (Astron Soc of the Pacific, San Francisco), Vol 213, pp 381–388.
4. Mader HM, Pettitt ME, Wadham JL, Wolff EW, Parkes RJ (2006) *Geology* 34:169–172.
5. Tung HC, Price PB, Bramall NE, Vrdoljak G (2006) *Astrobiology* 6:69–86.
6. Wettlaufer JS (1999) *Phys Rev Lett* 82:2516–2569.
7. Anderson DM (1967) *Nature* 216:563–566.
8. Hoekstra P, Miller RD (1967) *J Colloid Interface Sci* 25:166–173.
9. Pearson RT, Derbyshire W (1974) *J Colloid Interface Sci* 46:232–248.
10. Price PB, Sowers T (2004) *Proc Natl Acad Sci USA* 101:4631–4636.
11. Rüscher CH, Gall S (1995) *Phys Chem Min* 22:468–478.
12. Purwantini E, Daniels L (1998) *J Bacteriol* 180:2212–2219.
13. Sheridan PP, Miteva VI, Brenchley JE (2003) *Appl Environ Microbiol* 69:2153–2160.
14. Miteva VI, Sheridan PP, Brenchley JE (2004) *Appl Environ Microbiol* 70:202–213.
15. Karl DM, Bird DF, Björkman K, Houlihan T, Shackelford R, Tupas L (1999) *Science* 286:2144–2147.
16. Priscu JC, Adams EE, Lyons WB, Voytek MA, Mogk DW, Brown RL, McKay CP, Takacs CD, Welch KA, Wolf CF, *et al.* (1999) *Science* 286:2141–2144.
17. Carpenter EJ, Lin S, Capone DG (2000) *Appl Environ Microbiol* 66:4514–4517.
18. Christner BC, Mosley-Thompson E, Thompson LG, Zagorodnov V, Sandman K, Reeve JN (2000) *Icarus* 144:479–485.
19. Priscu JC, Christner BC (2004) in *Microbial Diversity and Bioprospecting*, ed Bull AT (Am Soc Microbiol Press, Washington, DC), pp 130–145.
20. Bulat SA, Alekhina IA, Blot M, Petit J-R, de Angelis M, Wagenbach D, Lipenkov VYa, Vasilyeva LP, Wloch DM, Raynaud D, Lukin V (2004) *Int J Astrobiol* 3:1–12.
21. Abysov SS, Poglazova MN, Mitskevich JN, Ivanov MV (2005) in *Life in Ancient Ice*, eds Castello JD, Rogers SO (Princeton Univ Press, Princeton), pp 240–250.
22. Yao T, Xiang S, Zhang X, Wang N, Wang Y (2006) *Global Biogeochem Cycles* 20:GB1004.
23. Ma LJ, Catranis CM, Starmer WT, Rogers SO (1999) *Mycologist* 13:70–73.
24. Willerslev E, Hansen AJ, Christensen B, Steffensen JP (1999) *Proc Natl Acad Sci USA* 96:8017–8021.
25. Kellogg DE, Kellogg TB (2005) in *Life in Ancient Ice*, ed Castello JD, Rogers SO (Princeton Univ Press, Princeton), pp 69–93.
26. Sambrotto R, Burckle L (2005) in *Life in Ancient Ice*, eds Castello JD, Rogers SO (Princeton Univ Press, Princeton), pp 94–105.
27. Starmer WT, Fell JW, Catranis CM, Aberdeen V, Ma L-J, Zhou S, Rogers SO (2005) in *Life in Ancient Ice*, eds Castello JD, Rogers SO (Princeton Univ Press, Princeton), pp 181–195.
28. Baker I, Cullen D, Iliescu D (2003) *Can J Phys* 81:1–9.
29. Barnes PRF, Wolff EW (2004) *J Glaciol* 50:311–324.
30. Bender M, Sowers T, Dickson M-L, Orchardo J, Grootes P, Mayewski PA, Meese DA (1994) *Nature* 372:663–666.
31. Chappellaz J, Brook E, Blunier T, Malaizé B (1997) *J Geophys Res* 102:26547–26557.
32. Zinder SH (1993) in *Methanogenesis*, ed Ferry FG (Chapman and Hall, New York), pp 129–206.
33. Anderson DM, Tice AR (1967) *Ecological Studies* (Springer, Berlin), Vol 4, pp 107–124.
34. Miller SL (1969) *Science* 165:489–490.
35. Lipenkov VYa (2000) in *Physics of Ice Core Records*, ed Hondoh T (Hokkaido Univ Press, Sapporo, Japan), pp 327–358.
36. Pauer F, Kipfstuhl S, Kuhs WF, Shoji H (1999) *J Glaciol* 45:22–30.
37. Uchida T, Mae S, Hondoh T, Lipenkov VYa, Duval P, Kawabata J-I (1994) *Proc NIPR Symp Polar Meteorol Glaciol* 8:140–148.
38. Raynaud D, Chappellaz J, Ritz C, Martinerie P (1997) *J Geophys Res* 102(C12):26607–26613.
39. Brook EJ, Sowers T, Orchardo J (1996) *Science* 273:1087–1091.
40. Haan D, Raynaud D (1998) *Tellus* 50B:253–262.
41. Davidson DW, Desando MA, Gough SR, Handa YP, Ratcliffe CI, Ripmeester JA, Tse JS (1987) *Nature* 328:418–419.
42. Sloan ED (1998) *Clathrate Hydrates of Natural Gases* (Dekker, New York), 2nd Ed.
43. Mohammadi AH, Anderson R, Tohidi B (2005) *Am Inst Chem Eng* 51:2825–2833.
44. Kirby TW, Lancaster JR, Fridovich I (1981) *Arch Biochem Biophys* 210:140–148.
45. Brioukhanov AL, Thauer RK, Netrusov AI (2002) *Microbiology* 71:281–285.
46. Smith JJ, Howington JP, McFeters GA (1994) *Appl Environ Microbiol* 60:2977–2984.
47. Sharma A, Scott JH, Cody GD, Fogel ML, Hazen RM, Hemley RJ, Huntress WT (2002) *Science* 295:1514–1516.
48. Westphal AJ, Snead C, Butterworth A, Graham GA, Bradley JP, Bajt S, Grant PG, Bench G, Brennan S, Pianetta P (2004) *Meteoritics Planet Sci* 39:1–12.
49. Marcy Y, Ouverney C, Bik EM, Lösekann T, Ivanova N, Garcia-Martin H, Szeto E, Platt D, Hugenholtz P, Relman DA, Quake SR (2007) *Proc Natl Acad Sci USA* 104:11889–11894.
50. Tung HC, Bramall NE, Price PB (2005) *Proc Natl Acad Sci USA* 10:18292–18296.
51. DiMarco AA, Bobik TA, Wolfe RS (1990) *Annu Rev Biochem* 59:355–394.
52. Edwards T, McBride BC (1975) *Appl Microbiol* 29:540–545.
53. Lin X-L, White RH (1986) *J Bacteriol* 168:444–448.